Journal of Rock Mechanics and Geotechnical Engineering 9 (2017) 648–658

Contents lists available at ScienceDirect

Journal of Rock Mechanics and Geotechnical Engineering

journal homepage: www.rockgeotech.org

Full Length Article

# Numerical modelling of pullout of helical soil nail

Saurabh Rawat, Ashok Kumar Gupta*

*Department of Civil Engineering, Jaypee University of Information Technology, Waknaghat, Solan, 173234, India*

ARTICLE INFO

*Article history:*
Received 22 September 2016
Received in revised form
5 December 2016
Accepted 8 January 2017
Available online 1 August 2017

*Keywords:*
Finite element
Helical soil nail
Pullout response
Plate spacing
Plate diameter
Failure mechanism

ABSTRACT

An investigation into the pullout response of helical soil nail using finite element subroutine Plaxis 2D is presented. The numerical modelling of actual pullout response is achieved by axisymmetric and horizontal loading condition. The effect of varying number of helical plates, helical plate spacing and helical plate diameter is studied to understand the pullout capacity behaviour. The failure surfaces for various helical soil nail configurations and their pullout mechanisms are also analysed and discussed. The pullout capacity is found to increase with increase in number of helical plates. The helical plate spacing ratio ($s/D_h$) and diameter ratio ($D_h/D_s$) are found to increase the pullout only up to a critical value. The response of helical soil nail using axisymmetric finite element simulation is found similar to the uplift behaviour of helical piles and helical soil anchors. In the absence of literature regarding numerical modelling of helical soil nail, simulation results are validated with uplift responses of helical piles and soil anchors. A good agreement in their comparative study for pullout response is also observed.



## 1. Introduction

Simulation of interaction between soil nail and soil is an important issue in modelling a soil-nailed system. This soil-structure interaction is studied in terms of pullout resistance or bond strength of the nails (Liu, 2003; Akiş, 2009). Zhou et al. (2011) developed a three-dimensional (3D) finite element (FE) model to simulate the pullout behaviour of a soil nail in compacted and saturated completely decomposed granite (CDG) soil nail pullout box under different overburdens and grouting pressures by using modified Drucker–Prager Cap model. The stress release variations surrounding the soil nail during drilling, grouting, saturation, and pullout were simulated by the FE modelling and compared with available test data. In their study, Zhou et al. (2011) concluded that the established finite element method (FEM) can well simulate the pullout behaviour and performance of a soil nail in field soil slope. A similar study on the pullout and failure mechanism of soil anchors was also carried out by Zhao and You (2014). Rawat and Gupta (2016a,b) studied the failure mechanism and performance of soil nail in model slope using two-dimensional (2D) FEM.

In order to achieve a sound soil nail-soil interaction, researchers have analysed the use of more rough surfaced soil nails or soil anchors (Frydman and Shaham, 1989; Lutenegger, 2009). More detailed studies in regard to this context have been carried out on the pullout capacity of either screw piles (Kurian and Shah, 2009) or helical screw piles (Rao et al., 1991). In the study conducted by Rao et al. (1991), the impact of number of helical plates on ultimate capacity in clay using model helical screw piles of 75 mm diameter in a bed of compacted clay was investigated. Rao et al. (1991) investigated the failure mechanism variation based on the spacing of the helix and the pile diameter ratio. Two different types of failures, intact cylinders of soil between helical plates for $s/D < 1.5$ and isolated plugs of soil around each helix for $s/D > 1.5$, were observed, where $s$ is the helical plate spacing, and $D$ is the diameter of helical plate. These observations led to the conclusion that the maximum capacity was attained when $s/D$ was between 1 and 1.5. Lutenegger (2009) presented field test data on the uplift capacity of helical piles in clay in comparison to estimated capacities using cylindrical failure and individual plate bearing mechanisms. The study implied that the failure mechanism assumed in design (cylindrical failure or individual plate bearing) ought to depend on $s/D$.

Several numerical studies have been carried out on the failure mechanism of helical piles, for example, Merifield (2011) used small strain axisymmetric FE simulations of the ultimate uplift capacity of cast-in-place, deeply embedded, horizontal, circular plates at varying $s/D$ to show that the mechanism changed from

* Corresponding author.
*E-mail address:* ashok.gupta@juit.ac.in (A.K. Gupta).
Peer review under responsibility of Institute of Rock and Soil Mechanics, Chinese Academy of Sciences.

http://dx.doi.org/10.1016/j.jrmge.2017.01.007

cylindrical shear to individual plate bearing failure at $s/D = 1.58$. It was also observed from this study that axisymmetric analyses did not consider the impact of the pile shaft and the installation process on the ultimate capacity of helical piles. Stanier et al. (2013) studied the effect of active length and helical plate ratio on a transparent synthetic soil using particle image velocimetry. They observed that the pile capacity is dependent on the active length and failure occurs in the form of a cylindrical surface failure. Using the partial factor method in FE analysis, it showed that the active length is governed by the number, spacing and size of individual helical plate. A total of 19 full-scale model tests were carried out to study the compression and uplift capacities of helical piles with installation effort (torque). The FE routine, Plaxis foundation, was used to validate the experimental work. The helical screw nails were simulated using 3 circular pitched bearing plates located at the depth three times the helical plate diameter. FE analysis was also used by Papadopoulou et al. (2014) to study the performance of helical piles under axial and horizontal loadings. The axial and tensile capacities were simulated under axisymmetric condition as a shell foundation. The studies were further extended to investigations on the effect of shear strength parameters and number of helical plates on the characteristic ultimate resistance of piles.

Plaxis 3D was also used for numerical verification of experimental results by Mittal and Mukherjee (2015). They conducted studies on multiple helix piles at different depths of embedment. The investigators also developed correlations between the ultimate compression capacities of multiple helix piles with single helix pile by mathematical formulations. Todeshkejoei et al. (2014) presented a 3D numerical analysis of the installation process for helical anchors in clay. Along with the application of torque-capacity correlation, the results from their analyses can be used to predict the relationship between installation torque and normal force as functions of helix pitch, roughness, and thickness.

In the present study, axisymmetric FE modelling is conducted for simulating pullout mechanism of helical soil nail by Plaxis 2D. From the literature review, it is clear that insufficient information is available with regard to helical soil nail modelling. The literature provides ample data for simulation of helical piles or helical soil anchors. It is also evident from Tan et al. (2008) that the pullout behaviours of soil nails can be well simulated by vertical pullout in axisymmetric condition available in Plaxis 2D package. The horizontal orientation is simulated by applying a horizontal load on the absorbent boundary to account for overburden acting when soil is pulled out horizontally. The literature review further suggests that researchers (e.g. Salhi et al., 2013; Knappett et al., 2014; Demir and Ok, 2015) have modelled helical piles and helical anchors using a similar concept in Plaxis subroutine. Studies based on such modelling techniques have been used to understand the pullout or uplift capacity of helical piles and anchors. Applying the accuracy of this existing modelling technique to actual behaviour, the variation in helical soil nail failure mechanism and pullout capacity with the number, spacing, and diameter of helical plates can be studied. From the literature review, it can also be concluded that the effect of overburden on pullout behaviours of helical soil nails is significant. However, experimental evidence by Tokhi et al. (2016) is the only available data in that context. The FE analysis of such experimental work can further enhance the understanding of pullout responses of helical soil nails.

## 2. Parametric analysis using finite element

### 2.1. Helical soil nail

In the present FE analysis, the helical soil nail used is made up of steel with bar geometry taken as per the available dimensions given in ASTM A615 (ASTM, 2002) for threaded nail bars (Lazarte et al., 2003). The diameter of the nail shaft ($D_s$) is 19 mm with a nominal unit weight of 2.24 kg/m. The helical plates are also considered to be made of steel with diameters varying from 26.6 mm to 83.6 mm. This variation of helical plate diameter is used in $D_h/D_s$ ratios for numerical modelling. All soil nail lengths are fixed to 15 cm as done in the experimental work by Rawat and Gupta (2016a), which is converted for simulation using scale of 1:50 (i.e. 1 cm in experiments equal to 0.5 m in modelling). Thus, the nail length of 7.5 m is utilised in FE analysis. The spacing of the helical plates used is varied with $s/D_h$ ratios to study its effect on helical nail pullout capacity. With the bottom helical plate fixed at 15 mm from the nail end, different depths of embedment of top helical plate is achieved by varying the spacing of the helical plates, which is used in the analysis for embedment ratio $H/D_h$. A typical helical soil nail modelled in FE analysis is shown in Fig. 1.

### 2.2. Isotropic hardening soil model

The soil parameters used in FE analysis are taken from the experimental work by Rawat and Gupta (2016a) on reinforced soil slopes. A well graded, isotropic sand size soil is used for constitutive modelling in Plaxis 2D. The soil is modelled as a hardening soil which yields in plastic straining due to soil expansion. The hardening of soil is subjected to shear and compression hardening. The input $E_{50}^{ref}$ is used to model the shear hardening due to the primary deviatoric loading which induces irreversible plastic strains. Irreversible plastic strains are also induced by compression obtained

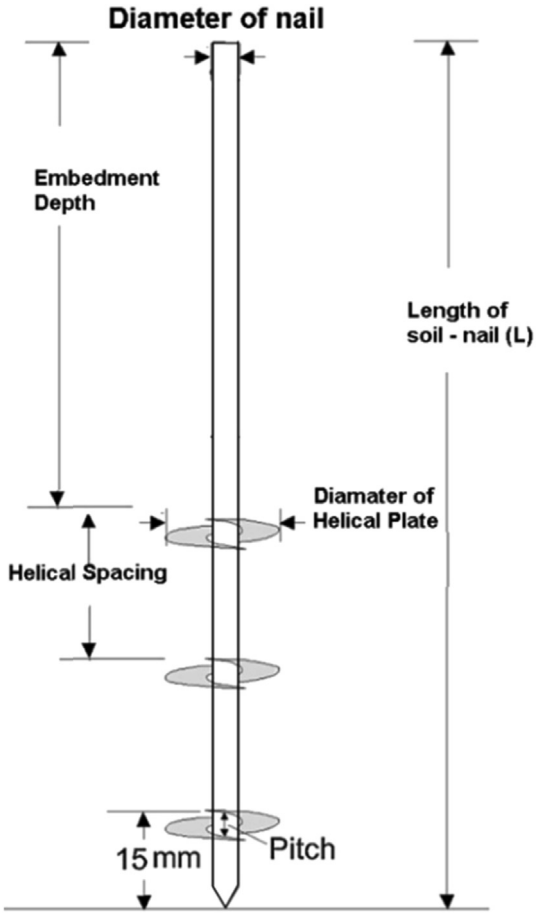


**Fig. 1.** Soil nail with helical plates modelled in FE analysis.

from oedometer loading and unloading test. The hardening of the soil is simulated by $E_{oed}^{ref}$ and $E_{ur}^{ref}$ input values in Plaxis 2D. The pullout test conditions are taken as drained with a low cohesion of 1.73 kPa and an angle of internal friction of 30°. No dilatancy is considered but tensile failure of soil along with shear failure is considered in the analysis. This is achieved by the use of tension cut-off value taken as 0 kPa for hardening soil model automatically by FE code. The soil parameters used for modelling are summarised in Table 1.

## 3. Numerical modelling of helical soil nail pullout

### 3.1. Pullout modelling in Plaxis 2D

In the present study, a FE subroutine Plaxis 2D is used for the numerical modelling of helical soil nail pullout behaviour. The pullout response modelling is carried out in accordance to the simulation done by Ann et al. (2004). The horizontal soil nail is simulated by a vertical inclusion in circular soil tank employing axisymmetric condition. The axisymmetric condition uses the *x*-axis as the radius and *y*-axis as the symmetrical axis of soil model. Plaxis 2D (Brinkgreve et al., 2012) emphasises the concept of using axisymmetric condition for simulation of cylindrical elements such as soil anchors, nails and piles as shown in Fig. 2. The below mentioned reasons are considered for 2D axisymmetric pullout modelling of helical soil nail:

(1) The change in stresses around a soil nail pullout is primarily due to the grouting pressure used during the installation procedure in conventional nails. Pradhan et al. (2006) concluded that the installation process of soil nail induced significant vertical stress changes in soil around the soil nails and that the soil nail pullout shear resistance is independent of the overburden pressure. Zhou et al. (2011) stated that "*It is well acknowledged that the soil nail pullout resistance is influenced by many factors, such as the installation method, overburden stress, grouting pressure, roughness of nail surface, soil dilation, degree of saturation, and soil nail bending*". Moreover, a similar observation by Hong et al. (2013) stated that "*It was found that the pullout resistance increased linearly with the grouting pressure, but the overburden pressure did not influence the pullout capacity*". Hence, the in situ stress conditions around the soil nail cannot be treated uniform. However, the installation of helical nails does not require any grouting procedure. The nails are penetrated into the soil by applying a torque at the nail head. This installation procedure is believed to produce minimal disturbance to surrounding soil. A similar conclusion was also derived by Tokhi et al. (2016) where it is stated that "*The design of new screw nail offers many advantages such as easy installation with no spoils and grouting, better nail ground interaction resulting in increased pullout capacity and its suitability for reinforcing all ground conditions including sand and gravel*". Since no spoils and grouting are expected with installation of helical nails, the in situ stresses can be assumed to be uniform around the helical nail. This assumption makes it reasonable to consider the helical nail pullout as an axisymmetric modelling problem.

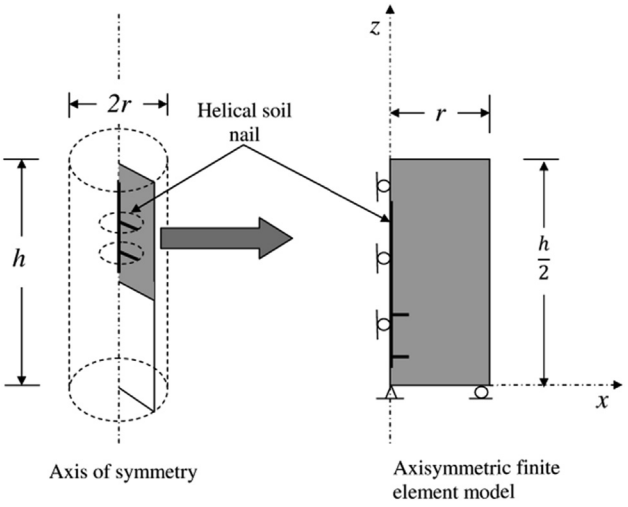


**Fig. 2.** Axisymmetric finite element model.

(2) The soil used in the present study has zero dilation corresponding to an angle of internal friction of 30°. Thus, the increased angle of internal friction and induced soil reaction pressure from the surrounding soil due to soil dilation (Luo et al., 2000) do not hold good for the present pullout of helical nail situation. This further confirms that stresses around the helical nail are uniform. Moreover, Luo et al. (2000) stated that "*The stress and strain near and within the rupture surface around a soil nail correspond to a triaxial strain problem, and the axial strain, $\varepsilon_a$, along the soil nail axial direction can be considered as constant*". Since triaxial strain problem can be treated as an axisymmetric 2D problem, a similar approach can also be made to analyse the pullout of helical nail by modelling it as 2D axisymmetric problem.

(3) The 2D axisymmetric pullout of soil nail analysis has also been carried out by Morris (1999). In that work, he stated that "*The boundary stresses in the vertical and horizontal directions are approximately equal, and the stresses in the soil immediately surrounding the soil nail may be nearly axisymmetrical, since the stress field here is dominated by the effect of the circular hole driven through the medium*". Similarly, Tei (1993) also concluded that as the relative stiffness between soil and nail increases, the axial stress distribution becomes more linear and shear stress distribution becomes more constant along the nail.

(4) Tokhi (2016) conducted 3D pullout of screw nails using an axisymmetric condition. As stated in his research, "*The pullout tests were simulated by an axisymmetric, 3D stress displacement elements model*". It is also found that the results of his 3D axisymmetric pullout analysis of new screw nail depict similar patterns of failure and stresses as those obtained from the present study of helical nails by 2D axisymmetric condition.

**Table 1**
Soil parameters used in Plaxis 2D (Rawat and Gupta, 2016a).

| Soil model type | Soil model condition | $\gamma$ (kN/m$^3$) | $\gamma_{sat}$ (kN/m$^3$) | $E_{50}^{ref}$ (MPa) | $E_{oed}^{ref}$ (MPa) | $E_{ur}^{ref}$ (MPa) | Poisson's ratio, $\nu$ | Cohesion, $c_{ref}$ (kPa) | $\phi$ (°) | $\psi$ (°) |
|---|---|---|---|---|---|---|---|---|---|---|
| Hardening soil | Drained, well graded sand | 17.3 | 19 | 30 | 30 | 90 | 0.3 | 1.73 | 30 | 0 |

Note: $E_{oed}^{ref}$ is obtained from oedometer (consolidation) tests conducted on sand used in the study, and $E_{50}^{ref}$ and $E_{ur}^{ref}$ are from standard consolidated drained (CD) triaxial tests on sand used in this study.

(5) The Plaxis practice manual given by Ann et al. (2004) also stated that "*Due to the characteristics of the axisymmetry model, the generated normal stress with the above mentioned method is uniformly distributed on the nail's perimeter. Although this initial stress condition is different compared to that of the actual working nail in which the circumferential normal stress distribution is non-uniform, caused by the difference in vertical and horizontal stresses, this shortcoming does not cause severe errors*".

Thus, keeping in view all the above-stated reasons, 2D axisymmetric modelling of pullout of helical nails can be employed to study the pullout mechanism with the assumption that no variation in initial stresses is expected in circumferential direction around the nail axis and helical plates are treated as circular disc with zero pitch along the nail shaft.

As discussed earlier, the constitutive soil modelling is carried out using a hardening soil model. The model dimensions are determined based on the effect of boundary conditions. The top and bottom boundary conditions are fixed in the vertical direction. The left boundary condition is simulated with a horizontal fixity whereas the right boundary condition is set free for application of overburden.

In order to avoid any boundary effect interference on the pullout mechanism, the right boundary is set at a distance of 60 times the nail radius (60$r$) from the axis of symmetry. To avoid confinement effects, care is taken to position the top boundary at a 20 times the nail radius (20$r$) from the nail head.

To model soil nail, an elastoplastic 15-noded plate element is used as suggested by Babu and Singh (2009). The helical plates are modelled by the same plate element as nail shaft. However, for practical design, helical plates are positioned on nail shaft at a particular angle and pitch. In this analysis, due to the restriction on simulation of helical pitch, the plates are taken horizontal to the shaft with zero pitch. The axial stiffness ($EA$) and the bending stiffness ($EI$) of the helical soil nail are taken as 28,355 kN/m and 0.64 (kN m$^2$)/m, respectively. The Poisson's ratio for the steel helical nails is taken as 0.2 with a unit weight of 2.24 kg/m.

The soil-nail interaction is simulated by constructing the interface between the nail shaft, nail helical plates and soil. Plaxis 2D code utilises a strength reduction factor ($R_{\text{inter}}$) to govern small displacements (elastic behaviour) and permanent slip (plastic behaviour) within the interface. The interface shear strength parameters are controlled by $R_{\text{inter}}$ by the following formulation (Brinkgreve et al., 2012):

$$c_{\text{interface}} = R_{\text{inter}}\, c_{\text{soil}} \tag{1}$$

$$\tan\phi_{\text{interface}} = R_{\text{inter}} \tan\phi_{\text{soil}} \tag{2}$$

The interface stiffness between soil and nail is handled by a virtual thickness "$t_{\text{interface}}$" which is automatically generated by FE subroutine. The $R_{\text{inter}}$ value used for current analysis is 0.67, which is adopted when no previous data are available for soil structure interaction. The numerical modelling parameters used in the analysis are given in Table 2.

The absorbent boundary placed at the right and bottom is to eliminate any spurious reflected waves. $\Sigma M_{\text{weight}} = 0$ is taken in the initial stress generation calculation step in order to avoid initial stresses generated by gravity, where $M_{\text{weight}}$ is the soil weight. The initial stress condition is created by imposing a surcharge load at the right boundary in the first step of calculation to create a uniformly distributed normal stress along the helical nail shaft to simulate the initial stress condition for the actual horizontally oriented nail. In this calculation step, the absorbent boundary is deleted, the upper and bottom boundaries are vertically fixed, the left boundary is totally fixed and the right boundary is totally free to allow the imposed load to be transferred to the nail shaft. This is done in order to achieve the actual pullout response of helical soil nail, wherein the effect of initial stress on a nail oriented horizontally is correctly simulated. All the other structural elements during the initial stress generation are deactivated. The soil overburden that must be acting on a horizontally oriented helical soil nail length is simulated by activating the uniformly distributed load of 7.3 kN/m$^2$ (Tan et al., 2008) on the right boundary of soil model. The earth pressure is generated as $K_o = 1 - \sin\phi$ having a value of 0.5. All the other structural elements during the initial stress generation are deactivated. The phreatic line is situated at the bottom of the model to create drained condition. The complete helical nail pullout model is shown in Fig. 3.

A small pullout force ($Q_0 = 10$ kN) is applied on the nail head to initialise the pullout. This initial pullout load is increased to an ultimate failure load by a load incremental factor $\Sigma M_{\text{load}}$ generated by Plaxis (Papadopoulou et al., 2014). Thus, the characteristic load at failure is calculated by

$$Q_p = \sum M_{\text{load}} Q_0 \tag{3}$$

The rate of load increment can be controlled by altering the additional step procedure available in the FE package. However, no simulation can be achieved for modelling the effects of helical nail installation by applying the initial torque. It is found from the literature review that installation torque alters the soil properties and hence the soil-nail interaction. Keeping this as a future scope of the present study, the analysis is carried out.

### 3.2. Modelling of different helical nail configurations

The helical nail configuration in the FE analysis is altered by using different diameters of helical plates with a constant shaft diameter of 19 mm. The $D_h/D_s$ ratio used are 1.4, 2.4, 3.4 and 4.4. The range for helix to shaft diameter is found to vary from 0 to 4.4

**Table 2**
Helical soil nail parameters used in numerical modelling.

| Nail type | Modulus of elasticity of nails, $E_n$ (GPa) | $\nu$ |
|---|---|---|
| Elastoplastic steel nails | 200 | 0.2 |

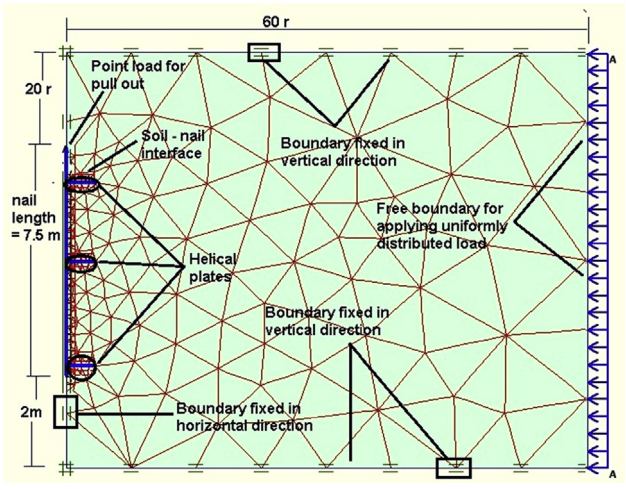


**Fig. 3.** Modelling of helical soil nail pullout.

(Knappett et al., 2014). The helical plate diameter calculated from $D_h/D_s$ ratio is 26.6 mm, 45.6 mm, 64.6 mm and 83.6 mm, respectively.

Throughout all the analysis, the bottom helix is fixed at a distance of 15 mm from the nail tip. The other helical plates are located at varying distances from the bottom helix. If top and bottom helical plates are used, it is treated as a double helical soil nail (2-H) and a combination of three helical plates at bottom, middle and top will serve as a multiple helical soil nail denoted as 3-H. The spacing of helical plates in 2-H and 3-H nails is calculated from the $s/D_h$ ratios. The spacing of helical plates is calculated for the maximum helical plate diameter of 83.6 mm corresponding to $D_h/D_s$ ratio of 4.4. These spacing values are determined to study the effect of $s/D_h$ ratios on the pullout capacity of helical nail and its failure response. With the change in the spacing, the embedment ratio ($H/D_h$) is also found to change. The behaviour of the helical anchors is found to vary with embedment ratio (Niroumand et al., 2012) and breakout factor – embedment ratio studies reported by Mitsch and Clemence (1985). The variations of helical plates carried out in FEM are summed up in Table 3.

Finally, the helical nail is also simulated as tapered helical nail by varying the diameter of top, middle and bottom helical plates with different $D_h/D_s$ ratios. Different combinations of bottom, middle and top helical plate diameters are used to constitute the tapered soil nail. A constant $s/D_h$ ratio of 2.5 is kept for the tapered nail. The diameters of 1-H, 2-H and 3-H nails are taken as $1.4D_s$, $2.4D_s$ and $3.4D_s$, respectively, as the first trial. These values of helical plate diameter are then varied between middle, top and bottom plates to model different tapered helical soil nail combinations.

## 4. Results and discussions

The results obtained from Plaxis 2D analysis for different types of helical nails, namely 1-H, 2-H, and 3-H, are compared with the existing literature. In the absence of direct results on helical soil nails, the comparison is done with helical soil anchors and helical piles to validate the results and trends.

**Table 3**
Different configurations of helical soil nails for Plaxis analysis.

| Configuration of helical plates | Notation | Number of helical plates | $D_s$ (mm) | $D_h$ (mm) | $s/D_h$ | $H/D_h$ | $D_h/D_s$ |
|---|---|---|---|---|---|---|---|
| 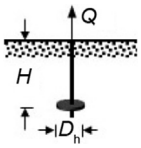 | 1-H | 1 | 19 | $4.4D_s$ | – | 1 | 1.4 |
| | | | | | | 2 | 2.4 |
| | | | | | | 3 | |
| | | | | | | 4 | 3.4 |
| | | | | | | 5 | |
| | | | | | | 6 | 4.4 |
| 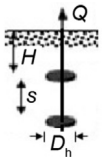 | 2-H | 2 | 19 | $4.4D_s$ | 1 | 1 | 1.4 |
| | | | | | 1.5 | 2 | 2.4 |
| | | | | | 2 | 3 | |
| | | | | | 2.5 | 4 | 3.4 |
| | | | | | 3 | 5 | |
| | | | | | 3.5 | 6 | 4.4 |
| 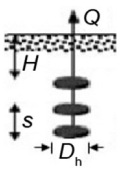 | 3-H | 3 | 19 | $4.4D_s$ | 1 | 1 | 1.4 |
| | | | | | 1.5 | 2 | 2.4 |
| | | | | | 2 | 3 | |
| | | | | | 2.5 | 4 | 3.4 |
| | | | | | 3 | 5 | |
| | | | | | 3.5 | 6 | 4.4 |

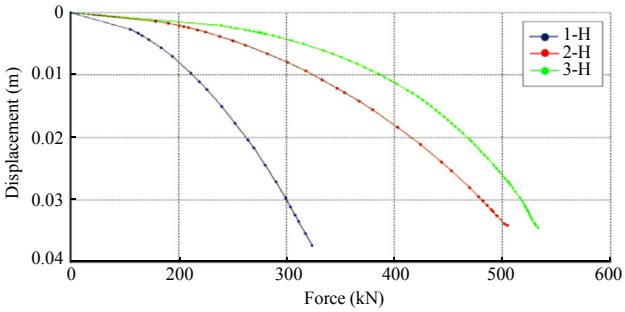


**Fig. 4.** Variation of pullout force with nail head displacement from Plaxis 2D.

### 4.1. Pullout behaviours of 1-H, 2-H and 3-H soil nails

Fig. 4 shows the pullout force against the displacement of nail head obtained from pullout model simulation in Plaxis 2D. From the FE plot, it can be observed that the pullout resistance of helical nail increases with increase in nail head displacement from its original position. A similar pattern as shown in Fig. 5 for pullout force vs. displacement is also observed from analytical and field investigations on multiple helix screw anchors carried out by Lutenegger (2009) and FE analysis by Papadopoulou et al. (2014) on helical micropiles. The FE analysis of present study depicts the fact that the pullout resistance of helical soil nail also increases with the number of helical plates. It is observed from Fig. 4 that as the number of helical plates increases from 1-H to 2-H and then to 3-H, a sufficient increase in helical nail pullout capacity is attained. As the helical plate is introduced along with the nail shaft, an increase in bearing area is achieved. The pullout resistance is governed by nail shaft-soil shearing and an increased surface area due to the helical plate. As the number of helical plates is increased from 1-H to 2-H, in addition to increased bearing area, soil between the helical plates gets compacted. This inter-helical soil densification increases the angle of internal friction of soil. Moreover, the inter-helical soil now starts to behave like a compacted block of soil. The cylindrical shear failure mechanism is thus dependent on the soil block-soil shearing resistance which is greater than nail shaft-soil shearing, thereby a significant increase in pullout force is achieved. As the number of helical plates increases from 2-H to 3-H, soil densification further increases. However, the pullout is still governed by shearing between inter-helical soil block and surrounding soil, i.e. cylindrical shear failure mechanism. Since only an additional shearing soil block is introduced in the mechanism, a smaller increase in pullout capacity of helical nail is observed from 2-H to 3-H as compared to that from 1-H to 2-H.

The increase in pullout capacity of 1-H helical nail with a shaft diameter of 19 mm and single helical plate diameter of 83.6 mm, 2-H helical nail with a shaft diameter of 19 mm and two helical plates

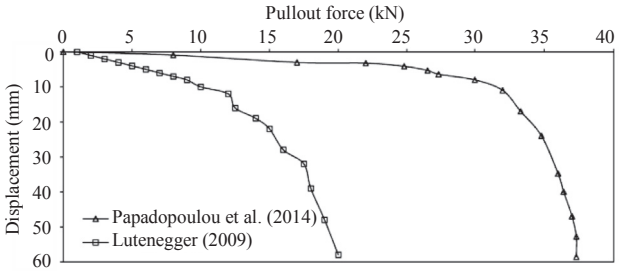


**Fig. 5.** Variation of pullout force with displacement from literature review.

diameter of 83.6 mm, respectively spaced at a distance of 250.8 mm apart, and 3-H helical nail with a shaft diameter of 19 mm and three helical plates diameter of 83.6 mm, respectively spaced at a distance of 250.8 mm apart, is shown in Fig. 6.

It is found that the pullout capacity is increased by 221.36% with the introduction of a single helical plate. A percentage increase in pullout of 1016.2% and 1211.87% is obtained for soil nails with double helical (2-H) and multiple helical (3-H) plates with diameters of $4.4D_s$ and spacing of 250.8 mm, respectively. Kurian and Shah (2009) also concluded that the percentage increase in ultimate tension load is 207% between smooth slip and no-slip screw piles with 900 mm diameter helical plates. It was also observed from their studies that increasing the diameter of the screw piles by introduction of helix can increase the ultimate pile strength by a large margin of 1240%.

The increase in pullout of helical soil nail with nail head movement can be accounted for by the fact that helical plates increase the bearing capacity due to the increase in overburden on helical plates. The increase in number of helical plates increases inter-helical soil densification. With this densification of soil, the angle of internal resistance of soil increases. To overcome this increased frictional resistance, a higher pullout force is required as more and more soil gets compacted with nail movement between the helical plates.

As the nail head starts to move, the pullout force varies linearly due to an elastic slip taking place between the interfaces under small displacements of 10%–14% of nail head displacement at failure. A transition phase is achieved thereafter which causes a nonlinear pullout force variation.

A relatively smaller increase in pullout is observed with large displacements of nail head. The reason for this variation is the occurrence of plastic-slip between the soil and nail. Due to this permanent slip, the pullout force at failure is achieved at larger nail head displacements as shown in Fig. 7. Tokhi et al. (2016) obtained the same shear force-displacement curves from laboratory tests carried out on screw soil nail.

### 4.2. *Effect of helical plate spacing on failure mechanism of helical soil nails*

The failure mechanism of helical soil nails is found to vary with the spacing of helical plates. The spacing of helical plates is determined by $s/D_h$ ratio ranging from 1 to 3.5. As seen from Fig. 8a, for

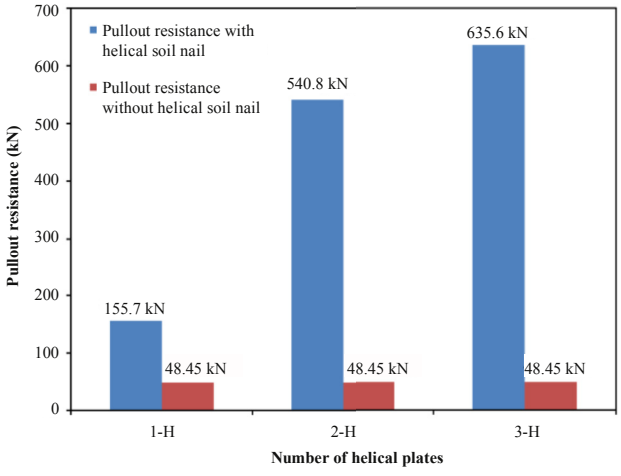


**Fig. 6.** Increase in the pullout capacity of helical nails with different numbers of helical plates.

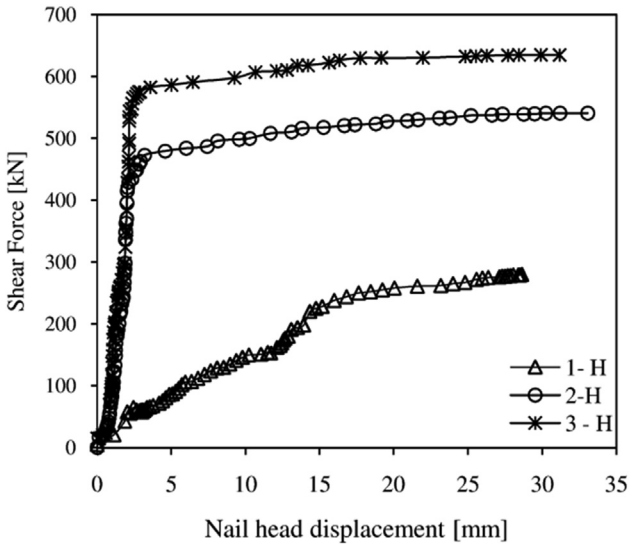


**Fig. 7.** Shear force variation with displacement of nail head.

1-H nails, an individual plate failure mechanism is found due to deep local failure of helical nail. Fig. 8b and c shows that in 2-H nail condition, the failure mechanism changes from deep global failure to deep local failure mechanism (Demir and Ok, 2015). The Plaxis analysis demonstrates that for all $s/D_h < 3$, cylindrical soil failure is observed for helical nail. This is due to the fact that soil gets compacted and starts to behave like soil block between helical plates. In 3D cases, it can be imagined as a cylindrical soil mass. The failure is governed by soil-to-soil shearing resistance between this cylindrical soil and adjacent soil.

As soon as the $s/D_h$ ratio increases beyond 3, the failure undergoes a transition from cylindrical shear failure to individual plate failure. In this case, the bearing of each plate acts separately, without affecting inter-helical soil. In 3-H nail, the increase in the number of helical plates from two to three reduces the embedment depth ($H$). This reduction in depth changes deep global failure to shallow failure as the failure is found to propagate to the ground surface. Thus, it can also be stated that there also exists a critical depth ($H_{cr}$) beyond which failure changes from deep to shallow. Moreover, this reduction in embedment depth with increase in helical plate spacing also leads to an individual plate failure as shown in Fig. 8d and e. Merifield (2011) observed similar failure patterns for different spacings of helical plates in soil anchors as shown in Fig. 9.

As seen from Tables 4 and 5, the pullout behaviour of helical nail changes with variation in helical plate spacing. Such variation in the uplift or tension capacity of helical piles and screw anchors has also been reported in the literature (Rao et al., 1991; Merifield and Sloan, 2006; Demir and Ok, 2015; Mittal and Mukherjee, 2015).

It is observed that the pullout capacity increases with increase in spacing between the helical plates. At $s/D_h < 3$, helical nails have failure surface which does not reach the ground surface. This deep global failure is characterised by the development of cylindrical shear failure mechanism. Individual plate failure is found to occur if the spacing is increased further, such that $s/D_h$ becomes greater than 3. The pullout capacity is found to increase by approximately 16% at $s/D_h > 3$ in contrast to that at $s/D_h < 3$, which brings about an increase of 19% in the pullout force for 2-H and 3-H nails. The comparison of pullout capacities obtained from FE analysis by Lutenegger (2011) as given in Fig. 10 suggests that the critical $s/D_h$ ratio is 3. However, a linear increase in the pullout capacity is observed from literature as well as from the current study. A small

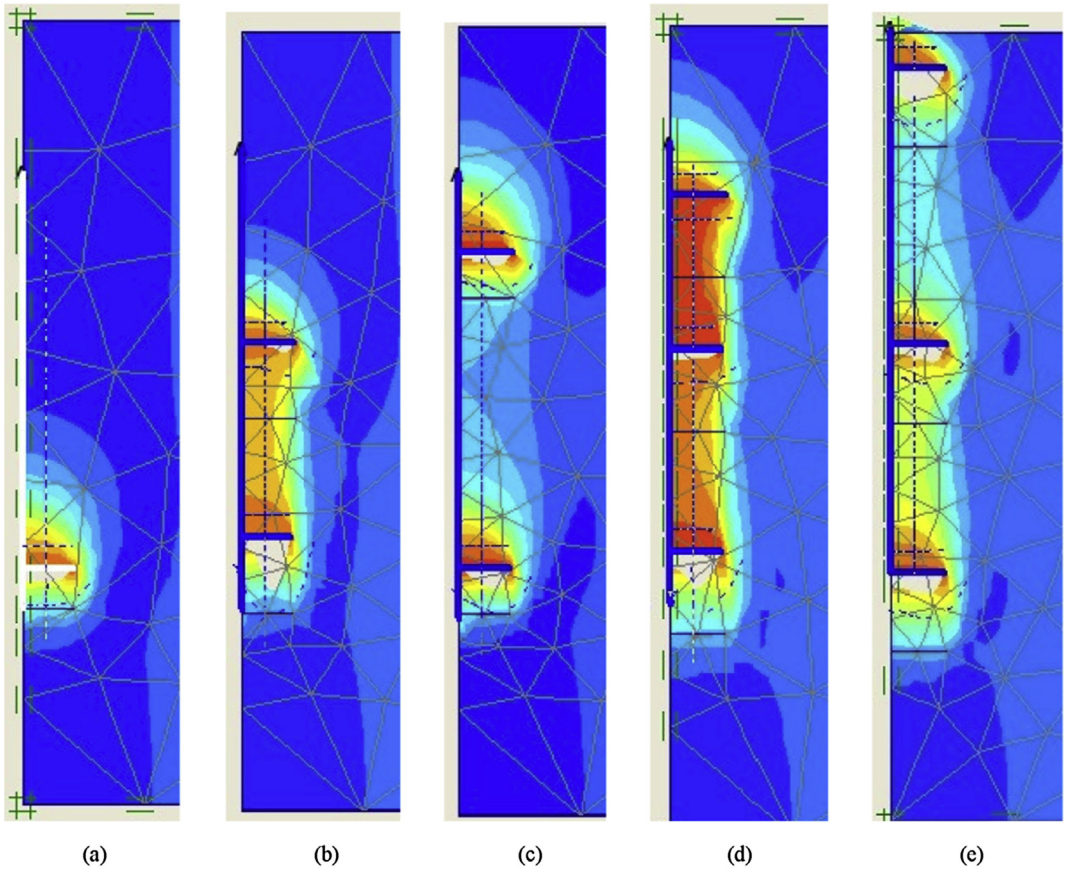


**Fig. 8.** Variations in failure mechanism with different spacings of helical plates: (a) 1-H; (b) 2-H at $s/D_h = 1.5$; (c) 2-H at $s/D_h = 3.5$; (d) 3-H at $s/D_h = 1.5$; and (e) 3-H at $s/D_h = 3.5$.

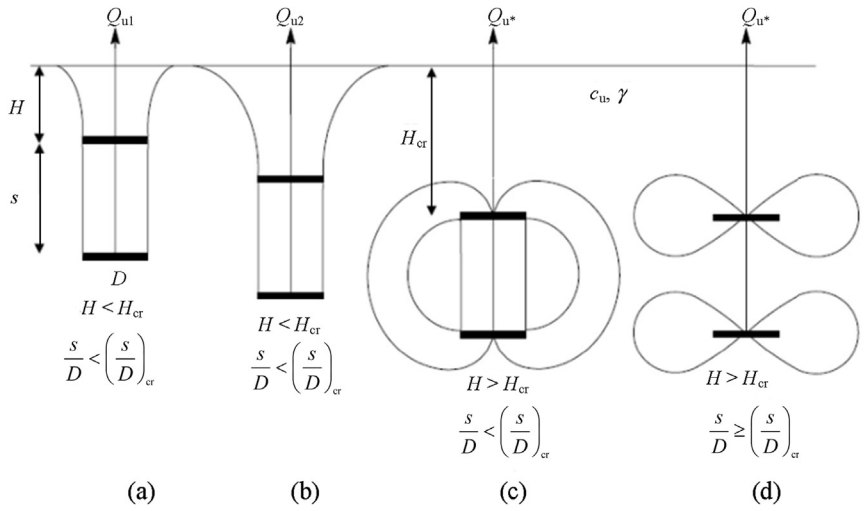


**Fig. 9.** Anchor behaviour: (a), (b) shallow failure mechanism; (c) global deep failure mechanism; and (d) local deep failure mechanism from Merifield (2011).

increase in the pullout results beyond the critical $s/D_h$ ratio was also reported by Lutenegger (2011).

With the increase in spacing between helical plates, the inter-helical soil begins to experience shaft friction in addition to helical plate bearing. This development of shaft friction is attributed to movement of inter-helical soil due to the increased spacing. The soil between closely spaced helical plates does not undergo sufficient movement during pullout. Thus, soil–soil interface provides the resistance against pullout along with helical plate bearing for all spacing less than the critical spacing. Beyond the critical spacing, this soil–soil interface friction changes to interface frictional resistance between nail shaft and inter-helical soil. This leads to an increase in pullout resistance with increased spacing.

To further enhance insight on this behaviour, several researchers have carried out studies in terms of a dimensionless parameter called breakout factor for helical piles and screw anchors. Mitsch and Clemence (1985) and then Ghaly et al. (1991) gave the breakout factor charts as function of embedment depth ratio. The

**Table 4**
Pullout force on 2-H nail with varying $s/D_h$ ratios (nail diameter $D_s$ = 19 mm, diameter of helical plate $D_h = 4.4D_s = 83.6$ mm).

| $s/D_h$ | Pullout resistance (kN) | $s/D_h$ | Pullout resistance (kN) |
|---|---|---|---|
| 1 | 180.71 | 2.5 | 450.67 |
| 1.5 | 271.07 | 3 | 540.8 |
| 2 | 360.53 | 3.5 | 631.11 |

**Table 5**
Pullout force on 3-H nail with varying $s/D_h$ ratios ($D_s$ = 19 mm, and $D_h = 4.4D_s = 83.6$ mm).

| $s/D_h$ | Pullout resistance (kN) | $s/D_h$ | Pullout resistance (kN) |
|---|---|---|---|
| 1 | 212.39 | 2.5 | 529.67 |
| 1.5 | 318.59 | 3 | 635.6 |
| 2 | 423.73 | 3.5 | 741.74 |

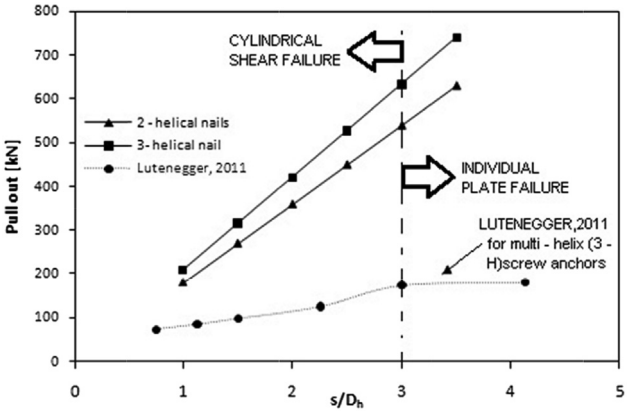


**Fig. 10.** Pullout force variation with different $s/D_h$ ratios.

embedment depth ratio is defined as the ratio of depth of top anchor to the diameter of top helical plate. The results of the present study are found to be in a good agreement with the results from literature, as shown in Fig. 11. The breakout factor is calculated from the formulation given by Das (1990):

$$[F_q] = \frac{Q_p}{\gamma' HA} \tag{4}$$

From Eq. (4), it can be seen that the breakout factor depends on the embedment depth ratio upto a point which reflects the critical value of $H/D_h$. It is observed in the present study that till $H/D_h > 3$, a linear increase in the breakout factor is found. Beyond this critical embedment ratio, $F_q$ is independent of embedment ratio. Sakr (2009) stated the critical embedment ratio from 4.4 to 7.8, whereas for the present analysis, it is 3. This underestimation of critical embedment ratio can be due to the failure of soil-nail interface under "immediate break away" condition. It can be seen from Fig. 8a–e that in each case, the soil below the helical plate is found to break away from the helical plate as shown by the white shading. This is due to the fact that the vertical stress below the plates reduces to zero and the helical plates are no longer in contact with the soil (Rowe and Davis, 1982).

From Fig. 11, it can be seen that the breakout factors for 1-H, 2-H and 3-H nails are found to increase with the embedment ratio. Similar trends of breakout factors were also observed by Mitsch and Clemence (1985) and Ghaly et al. (1991). The breakout factors are found to increase linearly up to an embedment ratio called the critical embedment factor. Beyond the critical embedment ratio,

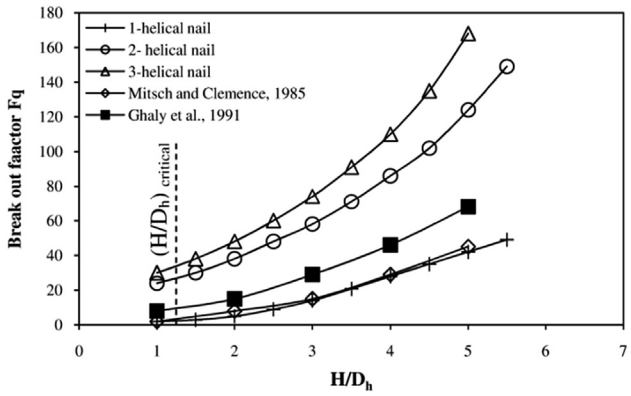


**Fig. 11.** Breakout factor variation with different embedment ratios.

the breakout factors follow a nonlinear pattern. It is also observed from Fig. 11 that the breakout factor increases with the increase in number of helical plates. Higher breakout factors are found for 3-H nail, followed by 2-H, and the lowest breakout factors are found for 1-H nail. The reason for this can be the transition of failure surface from shallow to deep global failure (Merifield, 2011).

The increase in breakout factor with the embedment ratio can also be accounted for because the bearing capacity of top helical plate reduces as the embedment ratio decreases. The reduction in overburden above the top helical plate decreases the pullout capacity and consequently a lower breakout factor is found. This can also be stated in context of soil nails as the soil near the nail head ahead of the helical plate reduces due to smaller embedment depth, rendering a smaller bearing and lower breakout factors.

### *4.3. Effect of helical plate diameter on pullout behaviour of helical soil nail*

The study conducted by Merifield (2011) suggested that the ratio of shaft diameter to plate diameter, which is less than 0.5, does not have significant effect on pullout capacity of helical anchors. In light of this observation, the ratio of nail shaft diameter to helical plate diameter selected for the present study is greater than 0.5 for all cases. It can be seen from Tables 6–8 that the pullout capacity of helical nail increases with the increase in $D_h/D_s$ ratios. This pattern of pullout increase is common for 1-H, 2-H and 3-H nail configurations. Based on this observation, one can also suggest that as the number of helical plates becomes greater, larger pullout capacities are observed with increasing shaft ratios.

**Table 6**
Pullout of 1-H nail with different $D_h/D_s$ ratios ($D_s$ = 19 mm).

| $D_h/D_s$ | Pullout resistance (kN) |
|---|---|
| 1.4 | 50.05 |
| 2.4 | 85.60 |
| 3.4 | 120.69 |
| 4.4 | 155.70 |

**Table 7**
Pullout of 2-H nail with different $D_h/D_s$ ratios ($D_s$ = 19 mm, and $s = 3D_h$).

| Spacing, $s$ (mm) | $D_h/D_s$ | Pullout resistance (kN) |
|---|---|---|
| 79.8 | 1.4 | 173.87 |
| 136.8 | 2.4 | 297.32 |
| 193.8 | 3.4 | 419.22 |
| 250.8 | 4.4 | 540.8 |

**Table 8**
Pullout of 3-H nail with different $D_h/D_s$ ratios ($D_s$ = 19 mm, and $s = 3D_h$).

| Spacing, $s$ (mm) | $D_h/D_s$ | Pullout resistance (kN) |
|---|---|---|
| 79.8 | 1.4 | 204.35 |
| 136.8 | 2.4 | 349.44 |
| 193.8 | 3.4 | 492.71 |
| 250.8 | 4.4 | 635.6 |

The reason for this increase in pullout capacity with helical plate diameter is the introduction of shaft friction that comes into play as the helical plate diameter is increased. The increase in plate diameter increases the bearing area of plates. At lower $D_h/D_s$ ratios and smaller spacing between helical plates, the shaft diameter reduces the helical plate bearing area. Since the spacing between the plates is small, cylindrical shear failure mechanism is predominant. This reduces the effect of shaft friction as no soil movement can take place between helical plates. The nail derives its pullout resistance completely by soil-to-soil interface friction.

However, with the increase in spacing, the increase in helical plate diameter enables shaft friction to mobilise during failure. Since the failure transits from cylindrical shear failure to individual plate failure, the soil between plates is able to move and mobilise the shaft friction. Though a reduction in helical plate bearing area is observed, the overall pullout resistance is now being derived from the bearing of helical plates and the mobilised shaft friction. Thus, with the increases in spacing and diameter of helical plates, the pullout resistance is found to increase.

An attempt is also made to find the effect of using a tapered helical soil nail on pullout capacity. The top, middle and bottom helical plates are modelled with helical plate diameter of $2.4D_s$, $3.4D_s$ and $4.4D_s$, respectively. A similar study was also carried out by Livneh and El Naggar (2008) on tapered tension piles.

Fig. 12a and b depicts a close match between the two studies. Livneh and El Naggar (2008) concluded that the uplift capacity of helical tension pile is not much affected by taper. However, the diameter of the upper helical shaft governs the uplift capacity. It

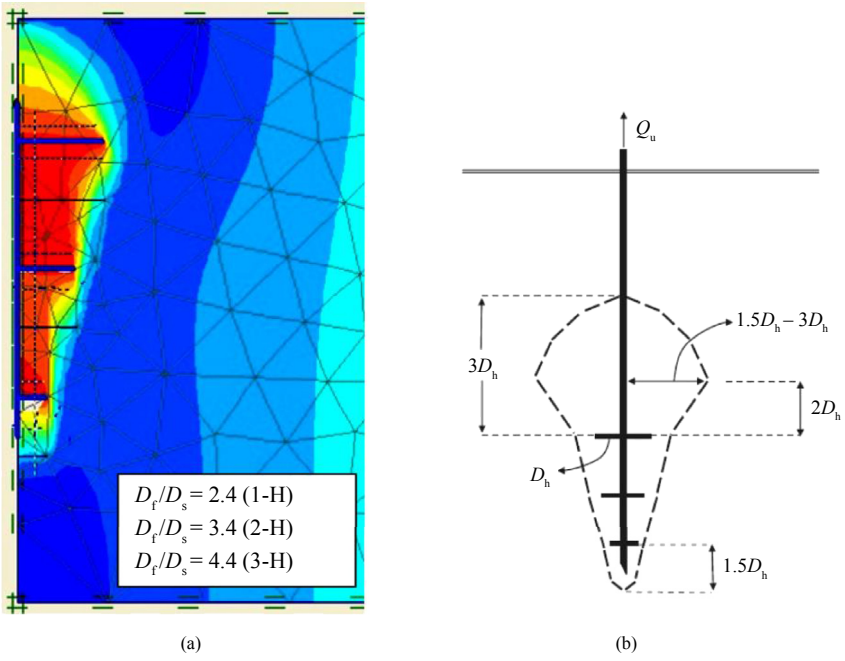


**Fig. 12.** Failure mechanisms of (a) helical soil nail in the present study, and (b) helical shaft piles in Livneh and El Naggar (2008).

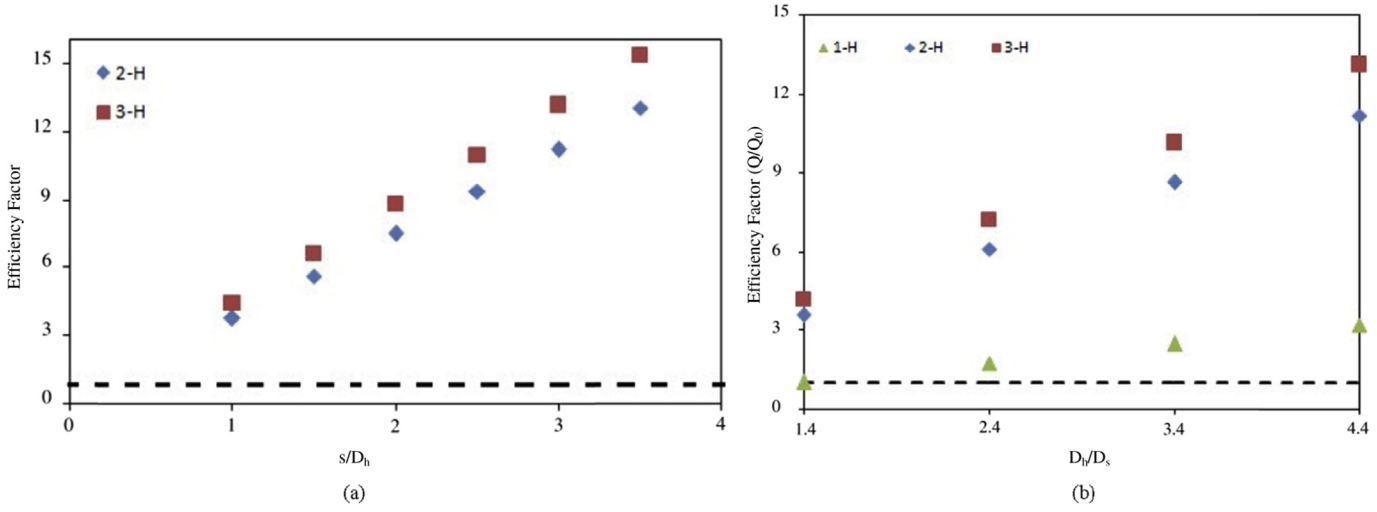


**Fig. 13.** Efficiency factors as a function of $s/D_h$ and $D_h/D_s$ ratios, respectively.

was inferred from their study that the bearing of the top helical plate and frictional resistance of inter-helical soil contribute to pile bearing capacity. A similar pattern of failure mechanism can also be suggested for helical soil nail by FE package Plaxis. However, any other finding on tapered helical soil nails is beyond the scope of present work.

### 4.4. Parametric analysis with variations in $s/D_h$ and $D_h/D_s$

The normalisation of multi-H soil nails pullout capacity with respect to pullout capacity of nail without helical plates is done in terms of a dimensionless factor known as efficiency factor ($Q/Q_0$). The effect of helical spacing variation shows that the efficiency factor increases with the increase in $s/D_h$ ratio. Moreover, higher increase in efficiency is observed for helical nails with larger number of helical plates, i.e. the efficiency of 3-H is greater than that of 2-H. Fig. 13a shows the variation in the efficiency factor ranging from 15 for 3-H nail to 13 for 2-H nail.

From Fig. 13b, it can be seen that the efficiency factor of helical soil nail also increases with the increase in $D_h/D_s$ ratio. The efficiency factor of 13.12 is observed for 3-H, followed by 11.16 for 2-H and a subsequently low value of 3.21 for 1-H. The high values for $Q/Q_0$ signify that increasing the number and diameter of helical plates has a significant effect on pullout behaviour of soil nail. Low value for single helical plate nail depicts that it has a pullout capacity as good as a nail without helical plate. This low efficiency factor of single helical nail can be attributed to the fact that the pullout capacity is derived largely by nail shaft in comparison to bearing offered by single helical plate. This signifies that the bearing of helical nail is more prominent in increasing pullout resistance as compared to interface friction between nail shaft and soil.

## 5. Conclusions

Based on the results of the present study from FE analysis by Plaxis 2D, the discussion and validation from literature, the following conclusions can be drawn:

(1) Plaxis 2D, a FE subroutine, can successfully be employed for simulation of helical nail with different nail configurations. As the results obtained from 2D axisymmetric modelling of helical soil nail in Plaxis 2D are found in accordance with results and observations made experimentally or analytically by researchers in the past. Moreover, the helical soil nail pullout behaviour is analogous to uplift of helical piles or helical screw soil anchors. The failure surfaces, load-displacement patterns and load transfer mechanism are found to be similar and in good agreement.

(2) The pullout capacity of helical soil nail increases with increase in number of helical plates. It can be concluded that the larger the number of helical plates, the larger the pullout capacity.

(3) Spacing of helical plates can significantly affect the pullout behaviour. The pullout increases as the spacing between helical plates increases. However, beyond a critical spacing ratio ($s/D_h = 3$), a smaller percentage increase in pullout is achieved. The spacing of helical plates also governs the transition of deep and local global failure mechanism to shallow failure mechanism. Cylindrical shear failure mechanism (deep global failure) is obtained for $s/D_h < 3$, while this failure changes to individual plate failure mechanism for $s/D_h > 3$.

(4) The dimensionless breakout factor ($F_q$) increases with the increase in embedment ratio. However, a critical embedment ratio ($H/D_h = 3$) is achieved beyond which the breakout factor is independent of $H/D_h$ variation. At this critical embedment ratio, transition in pullout failure mechanism from deep global failure (cylindrical failure) to deep local failure (individual plate) or shallow failure (individual plate) is observed. For the same variation in $H/D_h$, pullout is noticed to be on the higher end for nails with more number of helical plates.

(5) Pullout capacity of helical nail also increases with increase in $D_h/D_s$ ratio. For the same variation of $D_h/D_s$, nail with more number of helical plates reflects a higher pullout capacity. For decreased helical plate diameter of top, middle and bottom plates, the pullout capacity does not increase significantly in comparison to the same helical plate diameter for top, middle and bottom plate of nail.

(6) Dimensionless parameter called efficiency factor ($Q/Q_0$) increases with both $s/D_h$ and $D_h/D_s$ variations. The efficiency factor increases with increase in helical plate number on the nail for all variations of $D_h/D_s$.

## Conflict of interest

The authors wish to confirm that there are no known conflicts of interest associated with this publication and there has been no significant financial support for this work that could have influenced its outcome.

## Nomenclatures

| | |
|---|---|
| $D_s$ | Diameter of shaft of nail (mm) |
| $D_h$ | Diameter of helical plate on the nail (mm) |
| $L$ | Length of nail (m) |
| $H$ | Depth of the top helical plate from the nail head (m) |
| $s$ | Spacing between the helical plates (mm) |
| $A$ | Area of helical plate (m) |
| $E_{50}^{ref}$ | Reference stiffness modulus corresponding to reference confining pressure $p^{ref} = 100$ kPa (kPa) |
| $E_{oed}^{ref}$ | Oedometer loading modulus (kPa) |
| $E_{ur}^{ref}$ | Elastic unloading modulus (kPa) |
| $c_{ref}$ | Cohesion (kPa) |
| $Q_{pull}$ | Pullout capacity of helical nail (kN) |
| $R_{inter}$ | Reduction factor in Plaxis 2D |
| $E_n$ | Modulus of elasticity of nails (GPa) |
| $N_h$ | Number of helical plates |
| $s/D_s$ | Ratio of helical plate spacing to nail shaft diameter |
| $H/D_h$ | Ratio of top helical plate depth to helical plate diameter |
| $\phi$ | Angle of internal friction (°) |
| $\gamma$ | Unsaturated unit weight of soil (kN/m$^3$) |
| $\gamma_{sat}$ | Saturated unit weight of soil (kN/m$^3$) |
| $\psi$ | Dilatancy angle (°) |
| $\nu$ | Poisson's ratio |
| 1-H | Nail with a single helical plate |
| 2-H | Nail with double helical plates |
| 3-H | Nail with three helical plates |
| Multi-H | Nail with multi-helical plates |

## References

Akiş E. The effect of group behavior on the pull-out capacity of soil nails in high plastic clay. PhD Thesis. Middle East Technical University; 2009.
Ann T, Hai O, Lum C. Simulation of soil nail's dynamic pullout response. Plaxis Bulletin Issue 2004;15:10–2.
American Society for Testing and Materials (ASTM). Annual book of ASTM standards. ASTM; 2002.
Babu GLS, Singh VP. Simulation of soil nail structures using Plaxis 2D. Plaxis Bulletin 2009;25:16–21.
Brinkgreve RBJ, Engin E, Swolfs WM. Plaxis 2D 2012 user manual. Delft, Netherlands: Plaxis bv; 2012.
Das BM. Earth anchors. Amsterdam, Netherlands: Elsevier; 1990.

Demir A, Ok B. Uplift response of multi-plate helical anchors in cohesive soil. Geomechanics and Engineering 2015;8(4):615–30.
Frydman S, Shaham I. Pullout capacity of slab anchors in sand. Canadian Geotechnical Journal 1989;26(3):385–400.
Ghaly A, Hanna A, Hanna M. Uplift behavior of screw anchors in sand. I: dry sand. Journal of Geotechnical Engineering 1991;117(5):773–93.
Hong CY, Yin JH, Pei HF. Comparative study on pullout behaviour of pressure grouted soil nails from field and laboratory tests. Journal of Central South University 2013;20(8):2285–92.
Knappett L, Brown MJ, Brennan AJ, Hamilton L. Optimising the compressive behavior of screw piles in sand for marine renewable energy application. In: Proceedings of DFI/EFFC 11th international conference on piling and deep foundations. Deep foundations Institute; 2014.
Kurian NP, Shah SJ. Studies on the behaviour of screw piles by the finite element method. Canadian Geotechnical Journal 2009;46(6):627–38.
Lazarte CA, Elias V, Espinoza RD, Sabatini PJ. Geotechnical engineering circular No. 7 – soil nail walls. Report FHWA0-IF-03–017. Washington, D.C: US Department of Transportation, Federal Highway Administration; 2003.
Liu KX. Numerical modelling of anchor-soil interaction. PhD Thesis. National University of Singapore; 2003.
Livneh B, El Naggar MH. Axial testing and numerical modelling of square shaft helical piles under compressive and tensile loading. Canadian Geotechnical Journal 2008;45(8):1142–55.
Luo SQ, Tan SA, Yong KY. Pull-out Resistance mechanism of a soil nail reinforcement in dilative soils. Soils and Foundations 2000;40(1):47–56.
Lutenegger AJ. Cylindrical shear or plate bearing? – Uplift behavior of multi-helix screw anchors in clay. In: Contemporary topics in deep foundations: selected papers from the 2009 international foundation congress and equipment expo. New York: American Society of Civil Engineers (ASCE); 2009. p. 456–63.
Lutenegger AJ. Behavior of multi-helix screw anchors in sand. In: Proceedings of the 14th Pan-American conference on soil mechanics and geotechnical engineering, Toronto, Canada; 2011 (CD ROM).
Merifield RS, Sloan SW. The ultimate pullout capacity of anchors in frictional soils. Canadian Geotechnical Journal 2006;43(8):852–68.
Merifield RS. Ultimate uplift capacity of multiplate helical type anchors in clay. Journal of Geotechnical and Geoenvironmental Engineering 2011;137(7):704–16.
Mitsch MP, Clemence SP. Uplift capacity of helix anchors in sand. In: Uplift behavior of anchor foundations in soil. New York: ASCE; 1985. p. 26–47.
Mittal S, Mukherjee S. Behaviour of group of helical screw anchors under compressive loads. Geotechnical and Geological Engineering 2015;33(3):575–92.
Morris JD. Physical and numerical modelling of grouted nails in clay. PhD Thesis. University of Oxford; 1999.
Niroumand H, Kassim KA, Ghafooripour A, Nazir R, Chuan HS. Performance of helical anchors in sand. Electronic Journal of Geotechnical Engineering 2012;17:2683–702.
Papadopoulou K, Saroglou H, Papadopoulos V. Finite element analyses and experimental investigation of helical micropiles. Geotechnical and Geological Engineering 2014;32(4):949–63.
Pradhan B, Tham LG, Yue ZQ, Junaideen SM, Lee CF. Soil-nail pullout interaction in loose fill materials. International Journal of Geomechanics 2006;6(4):238–47.
Rao SN, Prasad YVSN, Shetty MD. The behaviour of model screw piles in cohesive soils. Soils and Foundations 1991;31(2):35–50.
Rawat S, Gupta AK. An experimental and analytical study of slope stability by soil nailing. Electronic Journal of Geotechnical Engineering 2016a;21(17):5577–97.
Rawat S, Gupta AK. Analysis of a nailed soil slope using limit equilibrium and finite element methods. International Journal of Geosynthetics and Ground Engineering 2016b;2(4):34.
Rowe RK, Davis EH. The behavior of anchor plates in sand. Geotechnique 1982;32(1):25–41.
Sakr M. Performance of helical piles in oil sand. Canadian Geotechnical Journal 2009;46(9):1046–61.
Salhi L, Nait-Rabah O, Deyrat C, Roos C. Numerical modeling of single helical pile behavior under compressive loading in sand. Electronic Journal of Geotechnical Engineering 2013;18:4319–38.
Stanier SA, Black JA, Hird CC. Modelling helical screw piles in clay and design implications. Proceedings of ICE-Geotechnical Engineering 2013;167(5):447–60.
Tan SA, Ooi PH, Park TS, Cheang WL. Rapid pullout test of soil nail. Journal of Geotechnical and Geoenvironmental Engineering 2008;134(9):1327–38.
Tei K. A study of soil nailing in sand. PhD Thesis. University of Oxford; 1993.
Todeshkejoei C, Hambleton JP, Stanier SA, Gaudin C. Modelling installation of helical anchors in clay. In: Oka F, Murakami A, Uzuoka R, Kimoto S, editors. Computer methods and recent advances in geomechanics. CRC Press; 2014. p. 917–22.
Tokhi H, Ren G, Li J. Laboratory study of a new screw nail and its interaction in sand. Computers and Geotechnics 2016;78:144–54.
Tokhi H. A study of new screw soil nail. PhD Thesis. Melbourne: RMIT University; 2016.
Zhao K, You CA. Influencing factors of shear stress distribution in anchoring interface. Electronic Journal of Geotechnical Engineering 2014;19:9675–86.
Zhou WH, Yin JH, Hong CY. Finite element modelling of pullout testing on a soil nail in a pullout box under different overburden and grouting pressures. Canadian Geotechnical Journal 2011;48(4):557–67.

**Dr. Ashok Kumar Gupta** is Professor and Head of Department of Civil Engineering, Jaypee University of Information Technology (JUIT), Waknaghat, Solan, Himachal Pradesh, India. He obtained his BSc degree from University of Roorkee (now IIT Roorkee), MEng degree from University of Roorkee in 1986, and PhD of Civil Engineering from IIT Delhi in 2000. His research covers testing and modelling of geotechnical materials, FE modelling and its applications to geotechnical engineering, continuum damage mechanics and its application to rockfill materials modelling, and engineering rock mechanics. He is Founder Chairman of Indian Geotechnical Society (IGS) Shimla Chapter.